Atmospheric Environment 147 (2016) 157–165

Contents lists available at ScienceDirect

Atmospheric Environment

journal homepage: www.elsevier.com/locate/atmosenv

# Thermophoretic capture of submicron particles by a droplet

Ao Wang, Qiang Song*, Qiang Yao

*Key Laboratory of Thermal Science and Power Engineering of Ministry of Education, Department of Thermal Engineering, Tsinghua University, 100084 Beijing, China*

## HIGHLIGHTS

- The available formula overestimates the thermophoretic capture efficiency.
- The relative deviation varies remarkablely with temperature difference and *Re*.
- Assumption of uniform particle concentration distribution leads to the deviation.
- A corrected formula for thermophoretic capture efficiency is established.

## ARTICLE INFO

*Article history:*
Received 29 June 2016
Received in revised form
1 September 2016
Accepted 4 October 2016
Available online 5 October 2016

*Keywords:*
Particulate matter
Droplet
Thermophoresis
Deposition efficiency

## ABSTRACT

Thermophoresis is an important mechanism for submicron particle capture by droplets. The thermophoretic deposition efficiencies under varying Reynolds (*Re*) numbers and temperature differences are obtained from the direct numerical simulation of the submicron particle flowing around the droplet. Comparison of the results calculated under the same conditions through the classical thermophoretic deposition efficiency formula and by numerical simulation shows that the Davenport formula always returns greater values than the numerical simulation, by a relative deviation of 19.8%–63.8%. The relative deviation decreased first and then increased with increasing difference in temperature, and increased gradually with increasing *Re*. The deviation resulted from the assumption that the particle concentration on the droplet surface is equal to that of the incoming flow in the formula deduction process. The convection of the gas and the thermophoresis of the particles together determined the migration of the particles in the boundary layer, and so determined the particle concentration distribution on the surface of droplets. Thus, the particle concentrations on the surface of droplets are actually lower than those of the incoming flow and are distributed bimodally on the surface. The dimensionless particle concentration on the surface of droplets decreased with increasing *Re*, and increased first then decreased later with increasing difference in temperature. The dimensionless thermophoretic driving velocity and *Re* were adopted to correct the formula. The results calculated by the corrected formula were consistent with the numerical simulation employed in this paper, such that the maximum relative deviation was reduced from the original 66.8% to less than 8%.



## 1. Introduction

Particulate matter is a critical pollutant in the atmospheric environment of many countries (Agudelo-Castaneda et al., 2013; Li et al., 2014). Fine particle pollution is becoming more stringent. Wet scrubbing and wet deposition are efficient methods of removing particles from industrial flue gas and from the atmosphere (Park et al., 2005; Queen and Zhang, 2008; Bae et al., 2010; Guo et al., 2014). Particle capture by a single droplet is the foundation of both processes (Jaworek et al., 2006); studies on single droplet capture are significant for developing industrial wet scrubbing technologies and understanding the capacity and mechanisms of wet deposition in the atmospheric environment.

In wet deposition and wet scrubbing processes, particle-carrying gas flows around the droplet. Particles can collide with the droplet surface during flow, under inertia, interception, Brownian mechanism, electrostatic mechanism, diffusiophoresis and thermophoresis (Kraemer and Johnstone, 1955; Pranesha and Kamra, 1996; Chate and Murugavel, 2011; Carotenuto et al., 2010). The single droplet efficiency is a basic input parameter in predicting

* Corresponding author.
*E-mail address:* qsong@tsinghua.edu.cn (Q. Song).

http://dx.doi.org/10.1016/j.atmosenv.2016.10.001
1352-2310/

the efficiency of wet deposition and wet scrubbing (Lee et al., 2006). For the convenience of calculation, the deposition efficiencies of single droplets under the effect of different capture mechanisms were organized to the empirical concise formula (Park et al., 2005). Deposition efficiencies are the function of dimensionless numbers in the capture process. The classical deposition efficiency calculation includes the following: the formula proposed by Slinn (1977), which is used for calculating the inertial deposition efficiency, interception deposition efficiency, and Brown diffusion deposition efficiency; and the thermophoretic deposition efficiency formula proposed by Davenport and Peters (1978). The total particle deposition efficiency of single droplets is the sum of the calculated deposition efficiencies under different mechanisms. Both the formulaic and numerical calculations of efficiency show that thermophoresis is the most important mechanism for submicron particle capture by droplets. Bae et al. (2009) estimated the relative contribution of thermophoresis in the wet deposition process through the thermophoretic deposition efficiency formula and found that the removal coefficient of 1-μm particles increased from $10^{-7}$ to $10^{-6}$ at 5 °C of temperature difference. In the industrial wet spraying process, a few degrees of temperature difference between the droplets and the gas results in a higher submicron particle deposition efficiency. Pilat and Prem (1976) performed a numerical simulation on the deposition efficiencies of single droplets on particles of different sizes as the temperature difference increases from 5 °C to 60 °C; the deposition efficiency of 1-μm size particles increased by two orders of magnitude, from 0.001 to 0.25, under the effect of thermophoresis.

The thermophoretic deposition efficiency formula proposed by Davenport and Peters (1978) is presently the only empirical formula for predicting the thermophoretic deposition efficiency of single droplets. Through experiments and numerical simulation, Wang et al. (1978) studied the deposition efficiency of droplets of 0.1 mm–1 mm size on 0.5-μm particles, under a 3 °C temperature difference between the environment and the droplet surface. Comparison between the experimental data and the predicted values by the Davenport thermophoretic deposition efficiency formula showed that the latter overestimated the former by a relative deviation of 24.1%–47.8%. Viswanathan (1999) performed a numerical simulation of the deposition efficiency of droplets on particles of 0.1 μm–1 μm size under a temperature difference of 10 °C–80 °C and with a droplet Reynolds number (*Re*) of 1.54–400 (characteristic size is the droplet diameter). The predicted values by the thermophoretic deposition efficiency formula (Davenport and Peters, 1978) were found to overestimate the numerical calculation results by 10%–50%. The classical deposition efficiency calculation is based on specific assumptions, theoretical analysis, and experimental data. Numerical simulation (Wang et al., 2015) of particle capture by single droplets show that the discrepancy between the research hypothesis and the actual process will likely result in deviations in the calculated values by the classical deposition efficiency formula and the actual values. Correction is needed based on the thermophoretic deposition behavior. The thermophoretic deposition efficiency of single droplets is the basis for analyzing industrial spraying and wet deposition process of fine particles. Further discussion should thus be made on the reason for the large deviation in the calculated value by the traditional thermophoretic deposition efficiency formula. A more accurate prediction method of the thermophoretic deposition efficiency of droplets is also urgently needed.

Previous literature (Wang et al., 2015) has studied the thermophoretically driven migration of submicron particles when flowing around droplets under different conditions by direct numerical simulation. Based on the simulated migration of submicron particles, the present paper reports the thermophoretic deposition efficiency of particles flowing around a droplet under different temperature differences and *Re* numbers. The differences between the results of direct numerical simulation and that calculated by the thermophoretic deposition efficiency formula are presented. The causes for the calculation error in the thermophoretic deposition efficiency formula are analyzed. A quantitative correction method applied to the thermophoretic deposition efficiency formula is put forward.

## 2. Governing equations and numerical method

### 2.1. Equations of particle motion and gas flow

In wet deposition and wet scrubbing processes, the gas that carries particles flows around the droplet as shown in Fig. 1. When the temperatures of the droplet and the atmospheric gas differ, the particles deviate from the streamline due to inertia, Brownian force, and thermophoretic force, causing the particles to collide with the droplet surface. The particles are assumed to be captured once they touch the droplet surface, which aligns with common wet deposition and wet scrubbing processes. The droplet is assumed to be a sphere with a constant diameter because the reduction in diameter from evaporation is negligible, actual deformation is slight in droplets with diameters less than 2 mm, and circulation inside the droplet is weak compared with outside flow (Pruppacher and Klett, 2010). The coordinate system is established with the center of the droplet as the origin. The equations of hydrodynamics can be expressed as follows:

$$\vec{\nabla}\cdot\vec{u} = 0 \tag{1}$$

$$\frac{\partial\vec{u}}{\partial t} + (\vec{u}\cdot\vec{\nabla})\vec{u} = -\frac{1}{\rho_f}\vec{\nabla}p + \nu\Delta\vec{u} \tag{2}$$

$$\frac{\partial T}{\partial t} + (\vec{u}\cdot\vec{\nabla})T = \frac{\lambda}{\rho_f c_p}\Delta T \tag{3}$$

where $t$ is the time, $\vec{u}$ is the gas velocity relative to droplet, $\rho_f$ is the density of gas, $p$ is the pressure, $\nu$ is the kinematic viscosity of gas, $T$ is the local gas temperature, $c_p$ is the specific heat capacity, and $\lambda$ is the thermal conductivity.

The particles in the gas flowing around the droplet are tracked by Lagrangian equation. As per the results of Pilat and Prem (1976), the thermophoretic force is two to three orders of magnitude greater than the Brownian diffusion force acting on submicron particles when the temperature difference is above 10 °C. Therefore, Brownian diffusion force is ignored in this study. The particle motion equation is given as:

$$m_p\frac{d\vec{v}}{dt} = \vec{F}_D + \vec{F}_T \tag{5}$$

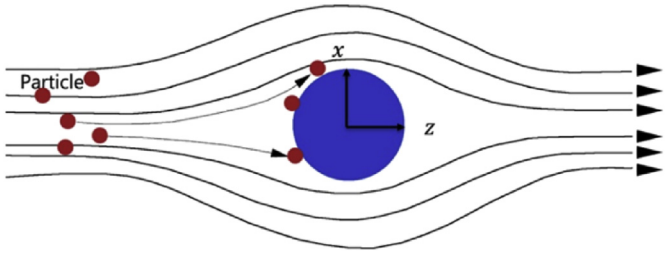


**Fig. 1.** Schematic diagram of the capture of particles by a droplet.

where $m_p$ and $\vec{v}$ are the mass and velocity of the particle center, respectively, the force $\vec{F}_D$ is the drag force, and $\vec{F}_T$ is the thermophoretic force.

As the *Re* of submicron particles is far less than 1, the drag force of a particle can well be approximated to the classical Stokes drag.

$$\vec{F}_D = \frac{3\pi\mu_g d_p}{C_C}\left(\vec{u} - \vec{v}\right) \tag{6}$$

where $\mu_g$ is the gas viscosity, $d_p$ is the particle diameter, $C_C$ is the Cunningham correction factor.

The thermophoretic force can be expressed as follows:

$$\vec{F}_T = \frac{3\pi\mu_g d_p}{C_C} C_T \tag{7}$$

$$C_T = -\frac{C_C}{3\pi\mu_g d_p} D_{T,p} \frac{1}{T}\frac{\partial T}{\partial r} \tag{8}$$

where $C_T$ is the thermophoretic velocity and $D_{T,p}$ is the thermophoretic coefficient, as suggested by Talbot et al. (1980).

### 2.2. Numerical methods and simulation parameters

In this study, a commercial Finite Volume Solver (ANSYS FLUENT V14.5) is used to solve the three-dimensional Navier–Stokes and energy equations of air and the motion equation of particle. The computational domain is shown in Fig. 2. The spherical droplet is placed closer to the inlet than to the outlet in the domain, and the wall is set as the boundary condition of the droplet. The air flows into the domain along the z-axis from the left plane (x, y). The inlet is set as the inlet boundary condition, and the pressure outlet is a free boundary condition for an unconfined flow, such as in the present simulation. The other surfaces in the domain are set as the wall boundary condition. The simulation method is the same with that in the literature.

For the simulation of flow around the droplet, structured meshes instead of easy-to-use unstructured meshes are employed because mesh quality has a significant influence on calculation accuracy. The domain has to be decomposed into several subdomains, such that the structured grid can be generated as in Fig. 3. The grids are structured and consist of body-fitted hexahedral control-volume elements (see Fig. 4).

The block effect of computational domain size and the resolution of grids influence the accuracy of flow simulation. The drag coefficient of flow around a droplet is usually used as an evaluative parameter. The accuracy of flow field simulation is tested by comparing the drag coefficient obtained by simulation with the experimental value. Thus, we calculate the drag coefficient under different domain sizes and grid resolutions. We select the most suitable domain sizes and grid resolutions for our simulation by comparing the drag coefficients determined in previous experiments performed under the same condition. Using the selected grids and the numerical method, the calculated drag coefficient and Nusselt number (*Nu*) correspond to the experimental results perfectly (Richter and Nikrityuk, 2012). The maximum relative deviation of drag coefficient and *Nu* in the calculation is within 5% in both the steady flow regime, which has a low *Re*, and the unsteady flow regime, which has a high *Re*. Hence, the flow field and temperature field around the droplet obtained via simulation is consistent with the actual flow field particle movement and temperature field.

Particles are injected uniformly into the domain from the projection of droplets on the inlet surface. The number of particles injected at once is 32,580. The DPM is used to track the position and motion of particles. The diameter of the particles is 0.1 μm. If the flow is in the unsteady regime, then the simulation of particle trajectory and the update of flow field are simultaneous. Under the condition of unsteady flow, we inject particles every three flow time steps during five flow periods to obtain an accurate average efficiency. The maximum number of particles injected into the computational domain is initially 3,258,000. After all particles are traced, the number of particles deposited on the droplet (divided by all particles to determine deposition efficiency) and the deposition location are analyzed statistically. The grid size is 10 μm in the simulation. In the DPM, the position of particle is calculated 20 times in every grid. The step length factor is 20. The time step of flow is $2 \times 10^{-5}$ s.

Apart from calculation by simulation, the traditional thermophoretic capture formula is also used to determine the thermophoretic deposition efficiency. This formula is the only equation that can be applied to predict the thermophoretic deposition efficiency. This formula, which was deduced by Davenport, is called Davenport thermophoretic deposition efficiency formula and is shown as follows:

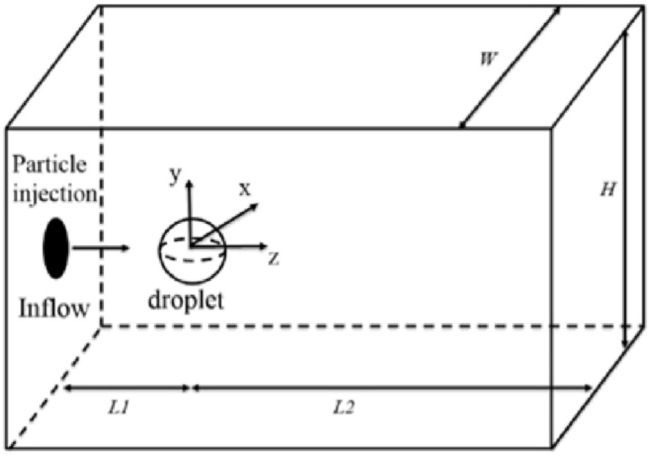


**Fig. 2.** Schematic diagram of the computation domain.

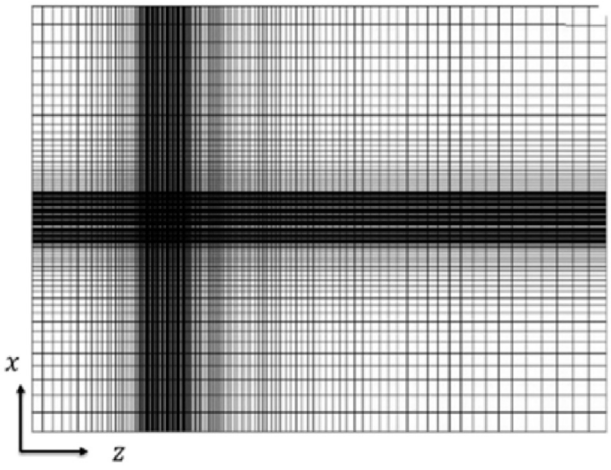


**Fig. 3.** Middle plane of computational grids. The flow direction is parallel to the z-axis and perpendicular to the x- and y-axis.

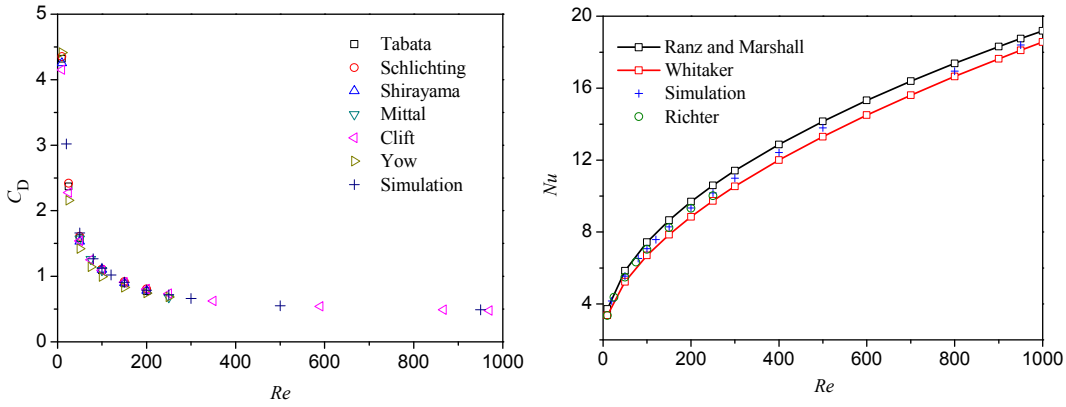


(a) Comparison of the drag coefficient (b) Comparison of the *Nu*

**Fig. 4.** Comparison of the drag coefficient and *Nu* obtained from experiments and that obtained from the present study.

$$E_{\text{Davenport}} = \frac{4D_{T,P}(2 + 0.6Re^{1/2}Pr^{1/3})\Delta T}{U_0 D} \quad (9)$$

where $U_0$ is the incoming velocity and $D$ is the droplet diameter.

Previous study (Wang et al., 2015) and the Davenport thermophoretic deposition efficiency formula both show that the thermophoretic deposition efficiency is mainly affected by the temperature difference between gas and droplet surface and *Re* of droplet. In the actual wet scrubbing and wet deposition process, the temperature difference is 10 °C–100 °C, the droplet diameter is 1 mm–2 mm, and the droplet *Re* is 250–950. In this paper, the temperature difference is set to 10 °C–100 °C, the droplet diameter is 2 mm, The droplet is set to the velocity ranging from 1.73 to 6.9 m/s. Thus, the droplet *Re* is set to 50 to 950 by changing the gas velocity.

## 3. Results and discussion

### 3.1. Thermophoretic deposition efficiency and relative deviation

Our previous work (Wang et al., 2015) demonstrated that particles flowing around a droplet are captured in two ways, through the action of thermophoretic force and through that of airflow. The first way is as follows. Particles that start near the axis of the droplet can easily enter the high temperature gradient region near the droplets with the action of thermophoretic force, allowing these to be captured by the droplet surface in front of the boundary layer separation point. The second way is as follows. Particles that start far from the axis of the droplet cannot be captured by the droplet surface in front of the boundary layer separation point, but are carried to the rear under the motion of the gas. Particles move to the back of the droplet and enter the trailing vortex due to thermophoretic force, then, as they are carried by the flow in vortex and into the high temperature gradient region near the back of the droplet, the particles are captured by the droplet at last. Fewer particles are captured through the second way than the first. When *Re* = 50 to 950, the number of particles captured by the second way is about 5%–12% of the total number of captured particles. The value of the temperature gradient determines the strength of the thermophoretic force, which depends on the *Re* of the flow around the droplet and the temperature difference. The role of the gas flow that carries around the droplets depends on the *Re* number. Temperature difference and *Re* are the key parameters in thermophoretic deposition efficiency.

The thermophoretic deposition efficiency when *Re* = 50 to 950 and the temperature difference is 10 °C–100 °C was calculated through the simulation method described above, and the result was compared with the results of the existing empirical formulas, as shown in Fig. 5. The solid points represent numerical results and the hollow points represent calculations through the Davenport formula under the same conditions. Fig. 5(a) shows that with the increase in the temperature difference between the external environment and the droplet surface, the thermophoretic force that the particles are subjected to increases, and the deposition efficiency increases. When *Re* = 500 and $\Delta T$ increases from 10 °C to 100 °C, the deposition efficiency increases from 0.00453 to 0.039. However, as the *Re* number increases, the deposition efficiency decreases, as shown in Fig. 5(b). For example, when $\Delta T$ = 100 °C and the *Re* number is increased from 50 to 950, the thermophoretic deposition efficiency decreases from 0.193 to 0.026. *Re* affects not only the flow around droplet, but also influences the temperature distribution around the droplet. For the first way of particle capture (which applies to the majority of particles), an increase in *Re* number makes the temperature boundary layer thinner, which causes an increase in temperature gradient, and at the same time increases the particle velocity. On the one hand, the thermophoretic force only exists in the thermal boundary layer around the droplet. The increase in the temperature gradient increases the thermophoretic force on the particles, and the velocity of the particles moving towards the droplet surface increases, leading to the time duration in which the particles move from out of the boundary layer to the surface movement shortened. On the other hand, when the carrying effect of the gas on the particle increases, the velocity of particles flowing with the gas increases, shortening the time duration in which the particles move through the same circumferential angle around the droplets, resulting in a short time in which thermophoretic force can act on the particle. The thermophoretic deposition efficiency is thus influenced by a combined effect of these two factors. The thermophoretic deposition efficiency decreases with *Re* number, which indicates that the shortness of the acting time of the thermophoretic force is a factor that controls the deposition efficiency. For particles captured through the second way, with the increase in *Re* number, the trailing vortex fixed on a certain position in the rear of the droplet sheds periodically, which carries some particles with it. The vortex shedding is unfavorable to the thermophoretic capture.

Comparing the results of the numerical simulation and the results from the Davenport thermophoretic deposition efficiency formula, a difference is seen between the two deposition

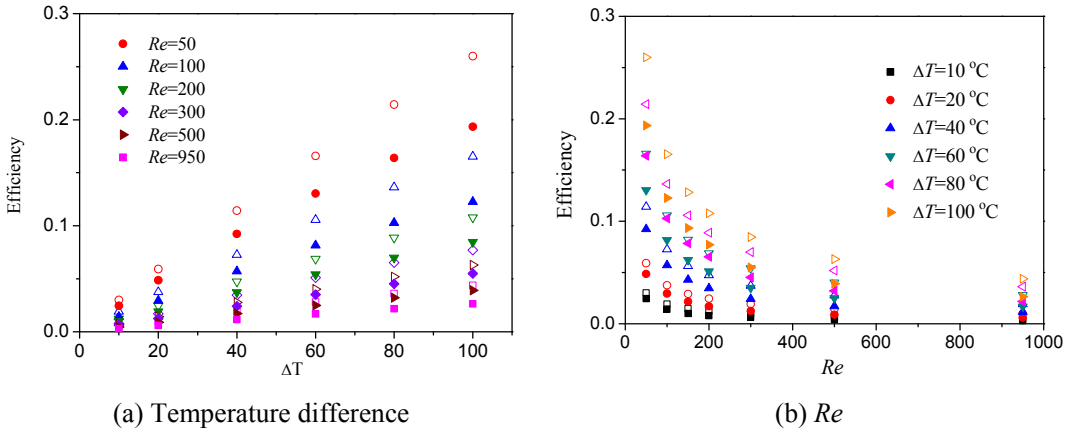


(a) Temperature difference (b) *Re*

**Fig. 5.** The thermophoretic deposition efficiency at different temperature differences and *Re* (the solid point represents numerical results and the hollow point represents results calculated from the Davenport formula).

efficiencies at the same temperature difference and *Re*; the value predicted by the Davenport formula is always higher than that predicted by the numerical simulation. The experimental results of Wang et al. (1978) showed the same trend and also had the same difference with the Davenport formula.

To characterize the difference between the empirical formula and the simulation results quantitatively, the relative deviation was defined as follows:

$$E_r = \frac{E_{\text{Davenport}} - E_{\text{sim}}}{E_{\text{sim}}} \tag{10}$$

where $E_r$ is the relative deviation, $E_{\text{Davenport}}$ is the thermophoretic deposition efficiency calculated from Davenport formula, $E_{\text{sim}}$ is the thermophoretic deposition efficiency obtained by the simulation described in this paper.

Fig. 6 shows the change in the relative deviation with the change in temperature difference and *Re*. As shown in Fig. 6 (a), as the temperature difference increases, the relative deviation initially increases and then decreases. For example, when $Re = 500$ and the temperature difference is increased from 10 °C to 100 °C, the relative deviation first decreases from 0.538 to 0.363 and then increases to 0.426. Fig. 6 (b) shows that, at a fixed temperature, the relative deviation gradually increases with increasing *Re*. For example, when the temperature difference is 80 °C and the *Re* number is increased from 50 to 950, the relative deviation gradually increases from 0.304 to 0.470. Thus, the relative deviation changes regularly with the temperature difference and *Re* number.

### 3.2. Theoretic analysis of relative deviation

The thermophoretic deposition efficiency was calculated from the formula $E = \dot{m}_{\text{deposit}}/\dot{m}_0$, where $\dot{m}_{\text{deposit}}$ is the number of particles deposited onto the surface of the droplets per unit time, and $\dot{m}_0$ is the number of particles coming from the projected area of the droplet at the entrance per unit time. $\dot{m}_{\text{deposit}} = \oint \alpha \frac{\partial T}{\partial r}\Big|_{r=r_0} \cdot n\mathrm{d}s$, where $\alpha \frac{\partial T}{\partial r}\Big|_{r=r_0}$ describes the thermophoretic velocity of particle at the droplet surface; because its direction is always towards the center of the droplet, the direction of the thermophoretic deposition of particles is also towards to the droplet center. $\alpha\,(\mathrm{m}^2/(\mathrm{K}\cdot\mathrm{s}))$ is a coefficient that characterizes the effect of thermophoretic force and is related to the physical property of particles and gas, $n$ is the particle concentration at the surface of the droplet, and $\mathrm{d}s$ is the area of droplet microelements. To obtain a simplified expression of the number of particle deposition on the droplet surface when

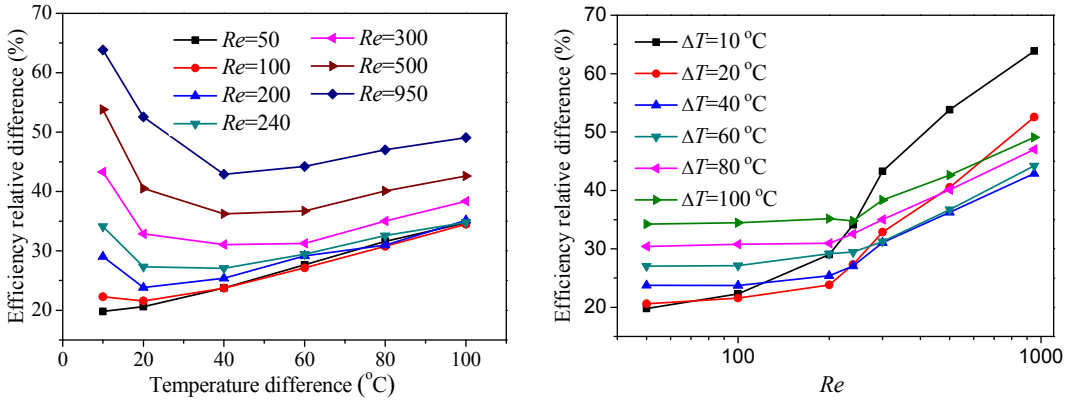


(a) Temperature difference (b) *Re*

**Fig. 6.** Change in relative deviation with temperature difference and *Re*.

deriving the thermophoretic deposition efficiency formula, Davenport expressed $n$ approximately as $n_0$, which is the concentration of particles at the incoming flow. The number of particle deposition on the droplet surface can then be reduced to $\dot{m}_{\text{deposit}} = n_0\alpha \cdot \oint \frac{\partial T}{\partial r}\Big|_{r=r_0} \mathrm{d}s$. $\oint \frac{\partial T}{\partial r}\Big|_{r=r_0} \mathrm{d}s$ is the amount of heat exchange on the droplet surface, which can be expressed in the empirical formula through the convective heat transfer coefficient and the temperature difference. Therefore, the number of particle deposition can be simplified as: $\dot{m}_{\text{deposit}} = n_0\alpha \cdot \pi D\Delta T \cdot Nu = n_0\alpha \cdot \pi D\Delta T(2 + 0.5Re^{1/2}Pr^{1/3})$.

However, the concentration of particles on the droplet surface is in fact different from the incoming flow. The gas temperature around the droplets change from the incoming flow temperature to the temperature of the droplet surface. The temperature gradient increases from out of the temperature boundary to the droplet surface, and the respective thermophoretic velocity increases, as shown in Fig. 7. Given that $Re = 150$ and the temperature difference is 100 °C, under the combined effect of convective transportation and non-uniform thermophoretic velocity, a distribution of particle concentration is seen in the vicinity of the droplet, such that regions closer to the surface of the droplet have a smaller particle concentration. Thus, the concentration of particles near the droplet surface is smaller than the particle concentration in the incoming flow, as shown in Fig. 8. This behavior explains why the Davenport formula overestimates the thermophoretic deposition efficiency.

Take the front stagnation point of the droplet as 0° and the back stagnation point of the droplet as 180°. Fig. 9 shows the distribution of the dimensionless particle concentration ($n/n_0$) on the droplet surface, which was calculated by dividing the particle concentration on the droplet surface to the particle concentration of the incoming flow; each data point has an average value within the range of 5° before and after this point. As seen from the figure, the dimensionless particle concentration on the droplet surface is less than 1, which means that the particle concentration on the droplet surface is smaller than the particle concentration of the incoming flow. The dimensionless particle concentration presents a regular distribution with a change in angle. The dimensionless particle concentration around the front stagnation point of droplet is between 0.6 and 0.8. With the increase in angle, the dimensionless particle concentration first increases, then decreases significantly and reaches its minimum value at around 125°–135°. The dimensionless particle concentration increases and decreases again when the angle is at 160°. The dimensionless particle concentration at the front portion of the droplet was found to be significantly higher than that at rear of the droplet. The point where the dimensionless particle concentration reaches its minimum value is the flow separation point under the corresponding $Re$ number (this position changes from 125° to 135°). The particle concentration distribution on the droplet surface is a result of the combined action of gas flow convection and the particle motion caused by thermophoretic force (Wang et al., 2015). The number of particle transport near the micro-element $\mathrm{d}s$ on a radial direction is $\mathrm{d}\dot{m} = \left(u_r + \alpha\frac{\partial T}{\partial r}\right)n\mathrm{d}s$. The nearer to the droplet surface, the smaller the $u_r$, and the weaker the flow convection. However, when temperature gradient gradually increases, the thermophoretic velocity increases, and thermophoretic transport is gradually enhanced. The number of particle transport to the droplet surface is $\mathrm{d}\dot{m}|_{r=r_0} = \alpha\frac{\partial T}{\partial r}\Big|_{r=r_0} n\mathrm{d}s$. The maximum temperature gradient is on the front stagnation point of the droplet. The temperature gradient decreases with the increase in angle, and the thermophoretic velocity decreases. The particle concentration increases as the number of particles transported to the droplet surface does not change much. However, as the angle further increases, because the temperature gradient is further reduced, the particle number transported to the vicinity of the droplet surface is significantly reduced, resulting in a decrease in particle concentration, until it reaches its minimum value in the vicinity of the flow separation point. After the flow separation point, because of the carrying action of the trailing vortex, the particle is transported back to the rear of the droplet, and the particle concentration increases again. At the same time, because the temperature gradient at the back stagnation point of the droplet is very large, the particle concentration decreases slightly at the back stagnation point.

Fig. 9 (a) shows the dimensionless particle concentration distribution at a temperature difference of 20 °C and with varying $Re$. The dimensionless particle concentration around the droplet surface is shown to decrease with increasing $Re$. This behavior occurs because when the $Re$ number increases, the temperature boundary layer becomes thinner, and temperature gradient in the temperature boundary layer increases, allowing the thermophoretic velocity $\alpha\frac{\partial T}{\partial r}\Big|_{r=r_0}$ acting on the particle near the droplet surface to increase. Meanwhile, the total number of particles $\dot{m}$ that can be transported to the surface decreases. As shown in Fig. 5 (b), when $Re$ increases, the thermophoretic deposition efficiency decreases. The equation $\dot{m} = \oint \alpha\frac{\partial T}{\partial r}\Big|_{r=r_0} \cdot n\mathrm{d}s$ indicates that the particle concentration on the droplet surface decreases. Thus when $Re$ increases, the relative deviation increases, as shown in Fig. 9 (a).

Fig. 9 (b) shows the dimensionless particle concentration distribution at $Re = 100$ and at varying temperature differences. This distribution is similar to that shown in Fig. 9 (a). However, when the temperature difference increases, the distribution of particle concentration at the droplet surface around the flow separation point (around 130°) follows a different rule. Fig. 9 (b) shows that as the temperature difference increases, the particle concentration before the separation point of droplet decreases. With increasing temperature difference, the number of particle transport $\dot{m}$ and $\alpha\frac{\partial T}{\partial r}\Big|_{r=r_0}$ before the flow separation point also increases, although the relative increase in value of $\dot{m}$ is less than the relative increase in value of $\alpha\frac{\partial T}{\partial r}\Big|_{r=r_0}$, leading to a decrease in particle concentration before the

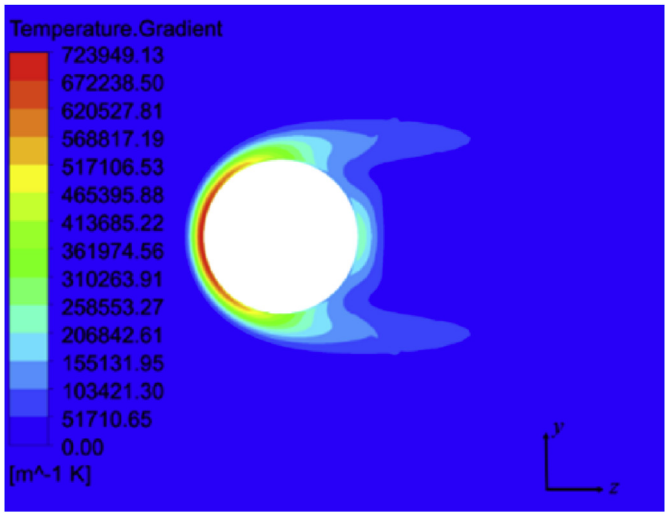


**Fig. 7.** The distribution of temperature gradient near the droplet surface ($Re = 150$).

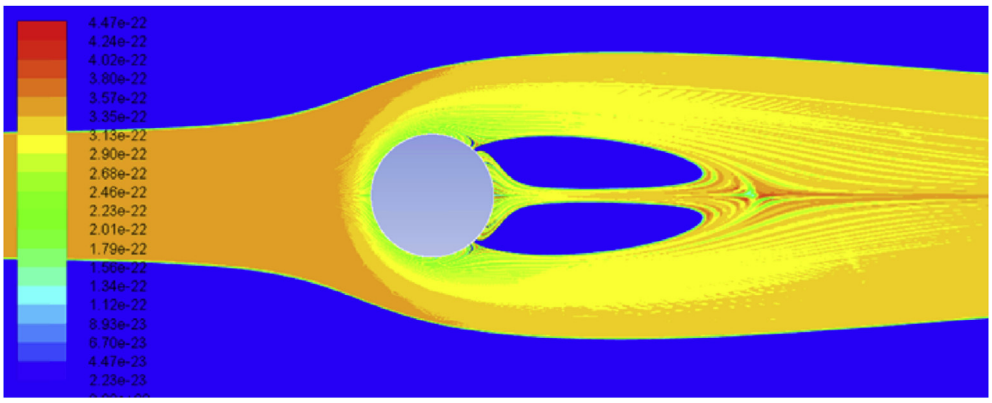


**Fig. 8.** Diagram of the particle concentration distribution as particles flow around the droplet.

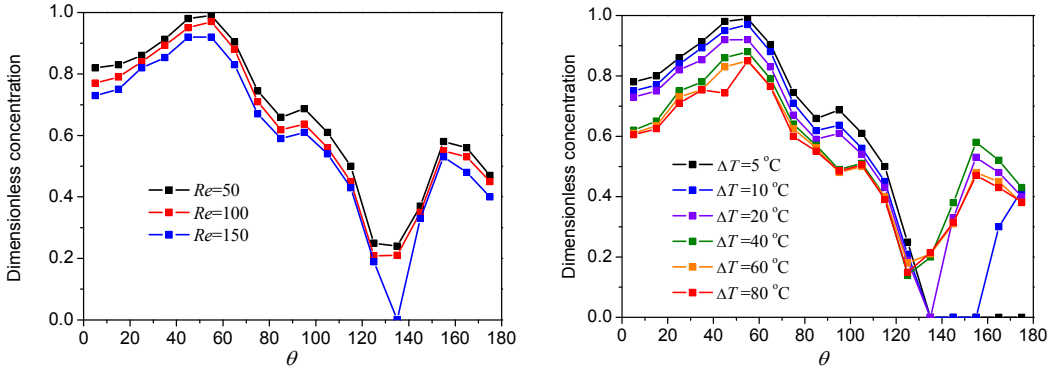


(a) The influence of *Re* on particle concentration distribution

(b) The influence of temperature difference on particle concentration distribution

**Fig. 9.** The dimensionless particle concentration distribution at the droplet surface.

flow separation point on the droplet surface. On the other hand, on the back of the droplet flow separation point, due to the increase in thermophoretic force, more particles are able to move to the rear of the droplets from the combined action of the trailing vortex and the thermophoretic force (Wang et al., 2015). The relative increase in value of $\dot{m}$ is larger than the relative increase in value of $\alpha\frac{\partial T}{\partial r}\Big|_{r=r_0}$ after the flow separation point, such that the particle concentration at the droplet surface after flow separation point increases. The average particle concentration at the droplet surface increases, and the relative deviation decreases with the increase in temperature difference. However, when the temperature difference is further increased, the relative increase in value of $\dot{m}$ is less than the relative increase in value of $\alpha\frac{\partial T}{\partial r}\Big|_{r=r_0}$ flow after the separation point, and the particle concentration on the back of the droplet decreases. Thus with the further increase in temperature, the relative deviation increases.

### 3.3. Amendment of relative deviation

In Sections 3.1 and 3.2, the change in the relative deviation of the thermophoretic deposition efficiency was calculated by simulation and through the Davenport formula, using *Re* and temperature difference as variables, after which the rule was analyzed. Temperature difference and *Re* changes the particle transport number and the thermophoretic velocity, then changes the distribution of particle concentration in the boundary layer, in the end affecting the relative deviation in thermophoretic deposition efficiency. The thermophoretic velocity is the key parameter in measuring the motion of particles towards the droplet (Guha, 2008). Therefore, in correcting for the calculation of deposition efficiency, the thermophoretic velocity was treated as a variable. To more accurately express the influence of thermophoretic velocity on the relative deviation and to facilitate the subsequent amendments in the relative deviation, the thermophoretic velocity was nondimensionalized with the incoming flow velocity, i.e., $u_{\text{thermo}}/u_0$. Deriving from the Davenport thermophoretic deposition efficiency formula, we can see that $E_{\text{Davenport}} = 4u_{\text{thermo}}/u_0$. Using $E_{\text{Davenport}}$ to represent the dimensionless thermophoretic velocity is helpful in establishing a relationship between $E_{\text{Davenport}}$ and the relative deviation, and is also convenient for the subsequent amendments in relative deviation.

The change in the relative deviation with *Re* and $E_{\text{Davenport}}$ is shown in Fig. 10. As can be seen from Fig. 10(a), for a given $E_{\text{Davenport}}$, an increasing *Re* gradually increases relative deviation and presents a linear relationship approximating the logarithmic value of *Re*. Fig. 10(b) shows the change in relative deviation with the dimensionless thermophoretic velocity. As can be seen from Fig. 10(b), for a given *Re* number, an increasing $E_{\text{Davenport}}$ initially increases then decreases the relative deviation. On the other hand, an increasing *Re* number shifts the curve upwards.

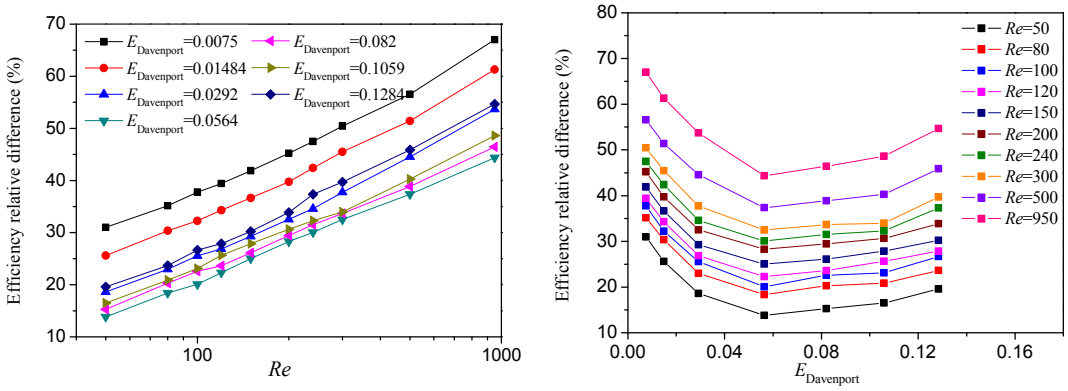


(a) $Re$ (b) $E_{\mathrm{Davenport}}$

**Fig. 10.** The change in the relative deviation with $Re$ and $E_{\mathrm{Davenport}}$.

Fig. 10 demonstrates how the relative deviation changes regularly with $Re$ and $E_{\mathrm{Davenport}}$. Fitting the experimental data and obtaining the following formula for the relative deviation of thermophoretic deposition efficiency:

$$E_{\mathrm{r}} = 0.275 \log_{10} Re + f(E_{\mathrm{Davenport}}) \tag{11}$$

where $f(E_{\mathrm{Davenport}}) = 33.26E_{\mathrm{Davenport}}^2 - 5.222E_{\mathrm{Davenport}} - 0.152$. The modified thermophoretic deposition efficiency is $E_{\mathrm{thermophoresis}} = E_{\mathrm{Davenport}}/(1 + E_{\mathrm{r}})$.

Based on the numerical simulation conditions of this article and Viswanathan (1999) and the experimental conditions of Wang et al. (1978), the thermophoretic deposition efficiency was calculated with the Davenport formula and the modified formula respectively. Fig. 11 shows the results, where the horizontal axis represents the numerical simulation results of this paper and Viswanathan (1999) and the experimental results of Wang et al. (1978), and the vertical axis represents the results calculated by the two efficiency formulas at the same conditions. The solid points are the results calculated from the corrected formula, the hollow points are the results calculated from the Davenport formula, the triangular points are the simulation results, the circular points are the results of the numerical simulation of Viswanathan (1999), and the square points are the results of the experimental simulation of Wang et al. (1978). The black line is a straight line with a slope of 1; the closer to the black line, the more consistent the predicted results of the formula with that of the experimental and direct numerical simulation. The modified thermophoretic deposition efficiency formula is shown to agree better with the experimental and numerical results; it reduces the maximum relative deviation of thermophoretic deposition efficiency from 66.8% to 8% for the conditions of this simulation, from 55.6% to 11.4% for the conditions of the numerical simulation of Viswanathan (1999), and from 47.8% to 9.32% for the conditions of the experiments of Wang et al. (1978). Thus, the modified formula can predict the thermophoretic deposition efficiency better for a droplet capturing particles.

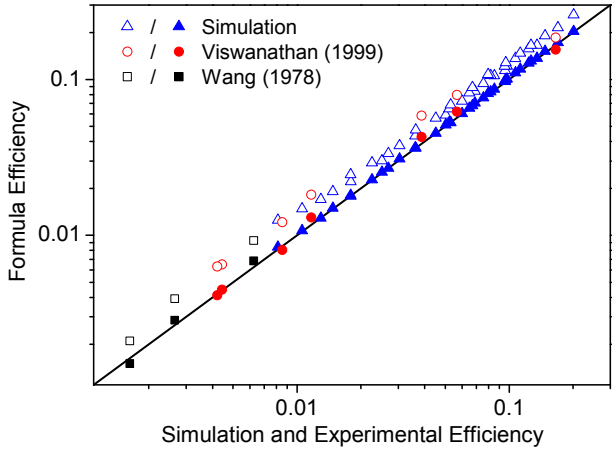


**Fig. 11.** The efficiencies values calculated by formula under simulation and experimental condition. (The solid points are the results calculated from the corrected formula, the hollow points are the results calculated from the Davenport formula; △: the simulation results in this paper, ○: the results of the numerical simulation of Viswanathan (1999),□: the results of the experimental simulation of Wang et al. (1978)).

## 4. Conclusion

The law of change in the particle thermophoretic deposition efficiencies of droplets under different $Re$ and temperature differences was obtained by direct numerical simulation. Increasing $Re$ enhanced the action of the gas on the downstream transport of particles and reduced the thermophoretic deposition efficiency. Increasing temperature difference increased thermophoretic strength and thermophoretic deposition efficiency. The deposition efficiency obtained through the thermophoretic deposition efficiency formula was 19.8%–63.8% higher than that obtained through numerical simulation. The relative deviation decreased initially then increased with the increase in difference in temperature, and also gradually increased with the increase in $Re$.

From the deduction process of the Davenport formula the deviation is found to be caused by the assumption that the particle concentration on the droplet surface is equal to that of the incoming flow. The particle concentrations on the actual surface of the droplets are actually lower than those of the incoming flow and are bimodally distributed on the surface. The dimensionless particle concentrations on the surface of droplets decreased with increasing $Re$, and increased first then decreased later with increasing difference in temperature. $Re$ and temperature difference are thus key parameters in determining the particle concentration on the surface of droplets. Increasing $Re$ decreased particle transport volume on the surface of droplets and increased the thermophoretic driving velocity, thus reducing the particle concentration on the surface of droplets. The difference in temperature increased both the particle transport volume on the surface of

droplets and the thermophoretic driving velocity. The competition between these factors determines the distribution of the particle concentration on the surface of droplets.

The dimensionless thermophoretic driving velocity and *Re* were adopted to correct the formula based on the law of change in the relative deviation with the key parameters, temperature difference and *Re*. The results calculated from the corrected formula were highly consistent with the numerical simulation and experimental results. The maximum relative deviation was reduced from the original 66.8% to less than 8%, which demonstrates that the corrected formula predicts the thermophoretic deposition efficiency more accurately.

## Acknowledgments

This work was supported by the fund from the National Natural Science Foundation of China (51576109) and the National Key Technologies R&D Program of China (2015BAA05B01).

## References

Agudelo-Castaneda, D.M., Teixeira, E.C., Rolim, S.B.A., Pereira, F.N., Wiegand, F., 2013. Measurement of particle number and related pollutant concentrations in an urban area in South Brazil. Atmos. Environ. 70, 254–262.

Bae, S.Y., Jung, C.H., Kim, Y.P., 2009. Relative contributions of individual phoretic effect in the below-cloud scavenging process. J. Aerosol Sci. 40, 621–632.

Bae, S.Y., Jung, C.H., Kim, Y.P., 2010. Derivation and verification of an aerosol dynamics expression for the below-cloud scavenging process using the moment method. J. Aerosol Sci. 41, 266–280.

Carotenuto, C., Nataleb, F.D., Amedeo, L., 2010. Wet electrostatic scrubbers for the abatement of submicronic particulate. Chem. Eng. J. 165, 35–45.

Chate, D.M., Murugavel, P., 2011. Below-cloud rain scavenging of atmospheric aerosols for aerosol deposition models. Atmos. Res. 99, 528–536.

Davenport, H.M., Peters, L.K., 1978. Field studies of atmospheric particulate concentration changes during precipitation. Atmos. Environ. 12, 997–1008.

Guo, L.C., Bao, L.J., She, J.W., Zeng, E.Y., 2014. Significance of wet deposition to removal of atmospheric particulate matter and polycyclic aromatic hydrocarbons: a case study in Guangzhou, China. Atmos. Environ. 83, 136–144.

Guha, A., 2008. Transport and deposition of particles in turbulent and laminar flow. Annu. Rev. Fluid Mech. 40, 311–341.

Jaworek, A., Balachandran, W., Krupa, A., Kulon, J., Lackowski, M., 2006. Wet electroscrubbers for state of the art gas cleaning. Environ. Sci. Technol. 40, 6197–6207.

Kraemer, H.F., Johnstone, H.F., 1955. Collection of aerosol particles in presence of electrostatic fields. Ind. Eng. Chem. 47, 2426–2434.

Lee, K.S., Lee, S.H., Park, H.S., 2006. Prediction for particle removal efficiency of a reverse jet scrubber. J. Aerosol Sci. 37, 1826–1839.

Li, Z.Q., Eck, T., Zhang, Y., Zhang, Y.H., Li, D.H., Li, L., Xu, H., Hou, W.Z., Lv, Y., Goloub, P., Gu, X.F., 2014. Observations of residual submicron fine aerosol particles related to cloud and fog processing during a major pollution event in Beijing. Atmos. Environ. 86, 187–192.

Park, S.H., Jung, C.H., Jung, K.R., Lee, B.K., Lee, K.W., 2005. Wet scrubbing of polydisperse aerosols by freely falling droplets. J. Aerosol Sci. 36, 1444–1458.

Pilat, M.J., Prem, A., 1976. Calculated particle collection efficiencies of single droplets including inertial impaction, Brownian diffusion, diffusiophoresis and thermophoresis. Atmos. Environ. 10, 13–19.

Pranesha, T.S., Kamra, A.K., 1996. Scavenging of aerosol particles by large water drops 1: neutral case. J. Geophys. Res. 101, 23373–23380.

Pruppacher, H.R., Klett, J.D., 2010. Microphysics of Clouds and Precipitation. Springer, Netherlands.

Queen, A., Zhang, Y., 2008. Examining the sensitivity of MM5-CMAQ predictions to explicit microphysics schemes and horizontal grid resolutions. Atmos. Environ. 42, 3856–3868.

Richter, A., Nikrityuk, P.A., 2012. Drag forces and heat transfer coefficients for spherical, cuboidal and ellipsoidal particles in cross flow at sub-critical Reynolds numbers. Int. J. Heat. Mass Tran. 55, 1343–1354.

Slinn, W.G.N., 1977. Some approximations for the wet and dry removal of particles and gases from the atmosphere. Water Air Soil Poll. 7, 513–543.

Talbot, L., Cheng, R.K., Schefer, R.W., Willis, D.R., 1980. Thermophoresis of particles in a heated boundary layer. J. Fluid Mech. 101, 737–758.

Viswanathan, S., 1999. Numerical study of particle collection by single water droplets. Ind. Eng. Chem. Res. 38, 4433–4442.

Wang, P.K., Grover, S.N., Pruppacher, H.R., 1978. On the effect of electric charges on the scavenging of aerosol particles by clouds and small raindrops. J. Atmos. Sci. 35, 1735–1743.

Wang, A., Song, Q., Ji, B.Q., Yao, Q., 2015. Thermophoretic motion behavior of submicron particles in boundary-layer-separation flow around a droplet. Phys. Rev. E 92, 063031.